Eu^{3+} reduction and efficient light emission in Eu_2O_3 films deposited on Si substrates

Gabriele Bellocchi,[1,2] Giorgia Franzò,[1,*] Fabio Iacona,[1] Simona Boninelli,[1] Maria Miritello,[1] Tiziana Cesca,[3] and Francesco Priolo[1,2]

[1]*MATIS CNR IMM, via Santa Sofia 64, 95123 Catania, Italy*
[2]*Dipartimento di Fisica e Astronomia, Università di Catania, via Santa Sofia 64, 95123 Catania, Italy*
[3]*Dipartimento di Fisica, Università di Padova, and CNISM, via F. Marzolo 8, 35131 Padova, Italy*
[*]*giorgia.franzo@ct.infn.it*

Abstract: A stable $Eu^{3+}\rightarrow Eu^{2+}$ reduction is accomplished by thermal annealing in N_2 ambient of Eu_2O_3 films deposited by magnetron sputtering on Si substrates. Transmission electron microscopy and x-ray diffraction measurements demonstrate the occurrence of a complex reactivity at the Eu_2O_3/Si interface, leading to the formation of Eu^{2+} silicates, characterized by a very strong (the measured external quantum efficiency is about 10%) and broad room temperature photoluminescence (PL) peak centered at 590 nm. This signal is much more efficient than the Eu^{3+} emission, mainly consisting of a sharp PL peak at 622 nm, observed in O_2-annealed films, where the presence of a SiO_2 layer at the Eu_2O_3/Si interface prevents Eu^{2+} formation.

©2012 Optical Society of America

OCIS codes: (160.5690) Rare-earth-doped materials; (250.5230) Photoluminescence.

References and links

1. A. Polman, "Erbium implanted thin film photonic materials," J. Appl. Phys. **82**(1), 366265 (1997).
2. M. Miritello, R. Lo Savio, F. Iacona, G. Franzò, A. Irrera, A. M. Piro, C. Bongiorno, and F. Priolo, "Efficient luminescence and energy transfer in Erbium Silicate thin films," Adv. Mater. (Deerfield Beach Fla.) **19**(12), 1582–1588 (2007).
3. K. Suh, M. Lee, J. S. Chang, H. Lee, N. Park, G. Y. Sung, and J. H. Shin, "Cooperative upconversion and optical gain in ion-beam sputter-deposited $Er_{(x)}Y_{(2-x)}SiO_{(5)}$ waveguides," Opt. Express **18**(8), 7724–7731 (2010).
4. M. Miritello, P. Cardile, R. Lo Savio, and F. Priolo, "Energy transfer and enhanced 1.54 µm emission in Erbium-Ytterbium disilicate thin films," Opt. Express **19**(21), 20761–20772 (2011).
5. M. Miritello, R. Lo Savio, P. Cardile, and F. Priolo, "Enhanced down conversion of photons emitted by photoexcited $Er_xY_{2-x}Si_2O_7$ films grown on silicon," Phys. Rev. B **81**(4), 041411 (2010).
6. X. Ye, W. Zhuang, Y. Hu, T. He, X. Huang, C. Liao, S. Zhong, Z. Xu, H. Nie, and G. Deng, "Preparation, characterization, and optical properties of nano- and submicron-sized Y_2O_3:Eu^{3+} phosphors," J. Appl. Phys. **105**(6), 064302 (2009).
7. G. Wakefield, E. Holland, P. J. Dobson, and J. L. Hutchison, "Luminescence properties of nanocrystalline Y_2O_3:Eu," Adv. Mater. (Deerfield Beach Fla.) **13**(20), 1557–1560 (2001).
8. H. Liang, Q. J. Zhang, Z. Q. Zheng, H. Ming, Z. C. Li, J. Xu, B. Chen, and H. Zhao, "Optical amplification of $Eu(DBM)_3$Phen-doped polymer optical fiber," Opt. Lett. **29**(5), 477–479 (2004).
9. D. Li, X. Zhang, L. Jin, and D. Yang, "Structure and luminescence evolution of annealed Europium-doped silicon oxides films," Opt. Express **18**(26), 27191–27196 (2010).
10. Y. C. Shin, S. J. Leem, C. M. Kim, S. J. Kim, Y. M. Sung, C. K. Hahn, J. H. Baek, and T. G. Kim, "Deposition of Europium Oxide on Si and its optical properties depending on thermal annealing conditions," J. Electroceram. **23**(2-4), 326–330 (2009).
11. L. Rebohle, J. Lehmann, S. Prucnal, A. Kanjilal, A. Nazarov, I. Tyagulskii, W. Skorupa, and M. Helm, "Blue and red electroluminescence of Europium-implanted metal-oxide-semiconductor structures as a probe for the dynamics of microstructure," Appl. Phys. Lett. **93**(7), 071908 (2008).
12. S. Prucnal, J. M. Sun, W. Skorupa, and M. Helm, "Switchable two-color electroluminescence based on a Si metal-oxide-semiconductor structure doped with Eu," Appl. Phys. Lett. **90**(18), 181121 (2007).
13. J. Qi, T. Matsumoto, M. Tanaka, and Y. Masumoto, "Electroluminescence of europium silicate thin film on silicon," Appl. Phys. Lett. **74**(21), 3203–3205 (1999).
14. M. Miritello, R. Lo Savio, A. M. Piro, G. Franzò, F. Priolo, F. Iacona, and C. Bongiorno, "Optical and structural properties of Er_2O_3 films grown by magnetron sputtering," J. Appl. Phys. **100**(1), 013502 (2006).

#160278 - $15.00 USD
Received 20 Dec 2011; accepted 3 Feb 2012; published 21 Feb 2012
(C) 2012 OSA

15. O. L. Krivanek, M. K. Kundmann, and X. Bourrat, "Elemental mapping by energy-filtered electron microscopy," Mater. Res. Soc. Symp. Proc. **332,** 341–350 (1994).
16. JCPDS Card No. 43–1009.
17. JCPDS Card No. 43–1041.
18. JCPDS Card No. 22–0286.
19. JCPDS Card No. 35–0299.
20. M. W. Shafer, "Preparation and crystal chemistry of divalent europium compounds," J. Appl. Phys. **36**(3), 1145–1152 (1965).
21. M. Nogami and Y. Abe, "Enhanced emission from Eu^{2+} ions in sol gel derived Al_2O_3–SiO_2 glasses," Appl. Phys. Lett. **69**(25), 3776–3778 (1996).
22. Y. Qiao, D. Chen, J. Ren, B. Wu, J. Qiu, and T. Akai, "Blue emission from Eu^{2+}-doped high silica glass by near-infrared femtosecond laser irradiation," J. Appl. Phys. **103**(2), 023108 (2008).
23. G. Gao, N. Da, S. Reibstein, and L. Wondraczek, "Enhanced photoluminescence from mixed-valence Eu-doped nanocrystalline silicate glass ceramics," Opt. Express **18**(S4 Suppl 4), A575–A583 (2010).
24. G. Bellocchi, G. Franzò, F. Iacona, S. Boninelli, M. Miritello, and F. Priolo, "Synthesis and characterization of light emitting Eu_2O_3 films on Si substrates," J. Lumin. (to be published).

1. Introduction

Rare earth compounds are currently attracting a growing interest in the field of photonics. Indeed, while the rare earth doping of suitable insulating or semiconducting host matrices has been considered for a long time the best approach to introduce light emitting impurities in Si-based materials [1], recently it has been demonstrated that the compound approach is able to overcome dopant clustering and precipitation, and therefore may open new and interesting perspectives for rare earth applications in photonics. Most of the recent efforts on these compounds have been focused on Er silicate thin films; relevant results include the observation of energy transfer between Si nanostructures and Er ions in Er silicate [2], the achieving of optical gain in Er/Y silicate waveguides [3] and the observation of a very efficient Er/Yb coupling in mixed silicates [4]. Furthermore, photon cutting phenomena, being of great relevance for photovoltaic applications of these materials, have been demonstrated in Er/Y silicates [5].

Among the various rare earths, a considerable attention is devoted to Eu, that presents an intense and stable emission in the visible region and has been successfully applied in phosphors and fiber amplifiers technologies [6–8]. Eu is stable in both its divalent (Eu^{2+}) and trivalent (Eu^{3+}) oxidation states. The photoluminescence (PL) spectrum of Eu^{3+} is characterized by several sharp lines at around 600 nm; on the other hand, Eu^{2+} emission is much stronger, being dipole-allowed, and is characterized by a broad peak, centered in the wavelength range 450-600 nm. These peculiar optical properties suggest for Eu-based materials interesting applications in Si photonics, provided that Eu-containing films can be synthesized and processed by using CMOS-compatible technologies. Several papers studied the optical properties of Eu-doped Si oxide [9] or Eu compound thin films [10], and the Eu emission properties have been exploited in light emitting devices based on Eu-doped SiO_2 [11,12] or Eu silicates [13].

In this work, we report an investigation on the properties of Eu_2O_3 films deposited on Si substrates. Annealing treatments in oxidizing and inert ambient allowed us to demonstrate a correlation between the structural and optical properties, and, in particular, to establish the conditions leading to a material exhibiting a very efficient room temperature (RT) light emission associated to the formation of Eu^{2+} ions.

2. Experimental section

Eu_2O_3 thin films were grown on (100) Si substrates heated at 400 °C by using an ultrahigh vacuum magnetron sputtering system. The base pressure was about 1×10^{-9} mbar. The deposition has been obtained by rf sputtering of a 4 inches diameter water-cooled Eu_2O_3 target (99.9% purity). The deposition was carried out with a sputter up configuration in a 5×10^{-3} mbar Ar atmosphere and a rf power of 200 W for 1 h. After deposition samples were thermally treated in O_2 or N_2 ambient by using a rapid thermal annealer. Transmission

electron microscopy (TEM) analysis in bright field (BF) mode, performed by a 200 kV Jeol 2010 microscope, was used to investigate the sample structure, while a 200 kV Jeol 2010F microscope, equipped with a Gatan Image Filter, was used to investigate the chemical composition by energy filtered TEM (EFTEM) analyses. Crystalline phases were identified by x-ray diffraction (XRD) measurements, performed with a Bruker-AXS D5005 diffractometer using a Cu Kα radiation with a grazing incidence angle of 1.0°. RT PL measurements were obtained by using a 325 nm He-Cd laser chopped through an acousto-optic modulator at a frequency of 55 Hz. The PL signal was analyzed by a single grating monochromator and detected by a Hamamatsu photomultiplier tube in the visible range. Photoluminescence excitation (PLE) measurements in the 250-500 nm range were performed by using a FluoroMax spectrofluorometer by Horiba.

3. Results and discussion

Figure 1(a) reports the BF cross-sectional TEM images of an as-deposited Eu_2O_3 film.

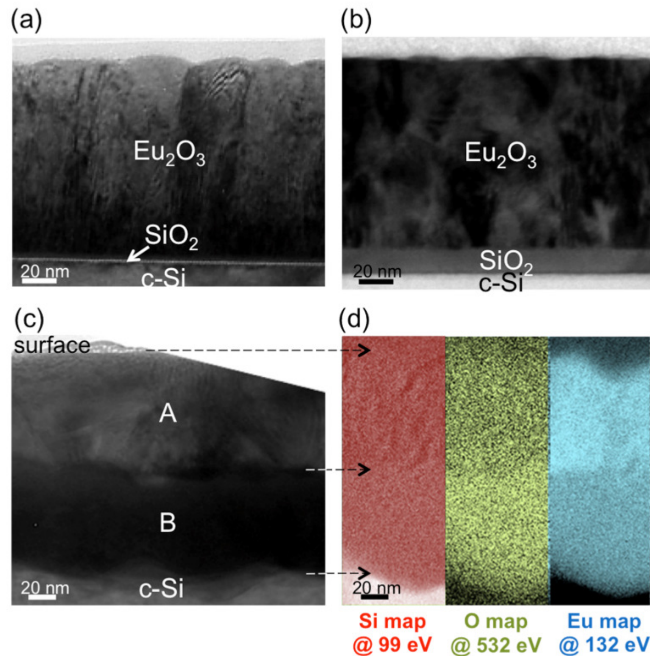

Fig. 1. (Color online) Cross-sectional TEM images of as-deposited and annealed Eu_2O_3 films. (a) BF image of an as-deposited film; (b) BF image of a film treated at 1000 °C for 30 s in O_2; (c) BF image of a film treated at 1000 °C for 30 s in N_2; (d) EFTEM maps of Si (on the left), O (in the middle) and Eu (on the right) of a film treated at 1000 °C for 30 s in N_2. EFTEM images refer to the same region of the sample. The arrows highlight the correspondence between the A and B sublayers in the TEM image shown in (c) and the regions with a different composition in the EFTEM images in (d).

The film is about 120 nm thick and exhibits a smooth interface with the Si substrate, where a thin SiO_2 layer (about 2 nm thick) is present. Figure 1(b) shows the BF cross-sectional TEM images of an Eu_2O_3 film annealed in O_2 at 1000 °C for 30 s. The process in oxidizing ambient increases the thickness of the interfacial SiO_2 layer up to about 15 nm and densifies the Eu_2O_3 film, the actual thickness being about 110 nm. EFTEM confirmed the composition of the layers shown in Figs. 1(a) and 1(b). Replacing O_2 with N_2 drastically changes the thermally-induced structural evolution of the film. Indeed, the BF TEM cross-section in Fig. 1(c) shows that, after a process performed at 1000 °C for 30 s in N_2, the Eu_2O_3 film becomes thicker (about 170 nm), and two sublayers, labeled in the figure as A (surface

#160278 - $15.00 USD Received 20 Dec 2011; accepted 3 Feb 2012; published 21 Feb 2012
(C) 2012 OSA

sublayer) and B (interfacial sublayer), can be distinctly recognized. EFTEM measurements indicate that no one of the two sublayers is pure SiO_2. In the absence of any interfacial SiO_2 layer, acting as diffusion barrier, the strong reactivity between Si and rare earth oxides is activated [14] and Si atoms can diffuse inside the film. This is demonstrated in Fig. 1(d), showing the Si, O and Eu chemical maps of the N_2-treated film, obtained by EFTEM. The images were taken by selecting electrons at 99 eV in the case of Si (corresponding to the $L_{II,III}$ edge), at 532 eV in the case of O (corresponding to the K edge) and at 132 eV in the case of Eu (corresponding to the N_{IV} edge) and by using the 3-windows method [15]. EFTEM data demonstrate that the interface between sublayers A and B evidenced by TEM corresponds to a quite abrupt variation of the concentration of the three elements. In particular, sublayer B is characterized by an appreciable Si concentration and has a higher O content and a lower Eu content than sublayer A.

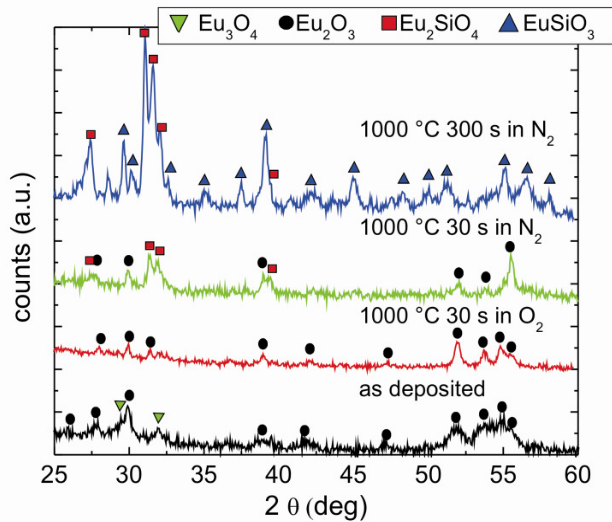

Fig. 2. XRD spectra of Eu_2O_3 films as-deposited, annealed at 1000 °C for 30 s in O_2, annealed at 1000 °C for 30 s in N_2 and annealed at 1000 °C for 300 s in N_2.

The crystalline structure of the films was studied by XRD. As shown in Fig. 2, the as-deposited film exhibits a diffraction spectrum mainly consisting of peaks belonging to the monoclinic Eu_2O_3 phase [16]. However, also a few peaks belonging to the sub-stoichiometric oxide Eu_3O_4, accounting for the oxygen deficiency which characterizes oxide films grown by sputtering, are identified [17]. The XRD spectrum of Eu_2O_3 annealed at 1000 °C for 30 s in O_2 shows only peaks corresponding to the Eu_2O_3 phase, suggesting the presence of a more ordered crystalline structure, due to a reduced defect density and to the restoration of a correct stoichiometry. The peaks are sharper than the ones of the as-deposited film, indicating an increased grain size. No Eu_3O_4-related peaks are found anymore. Figure 2 also reports the XRD spectrum of a film treated at 1000 °C for 30 s in N_2; peaks assigned to Eu_2O_3 are still present, but new peaks, corresponding to the monoclinic orthosilicate Eu_2SiO_4 [18], appear. The presence in the XRD spectrum of two different crystalline compounds (Eu_2O_3 and Eu_2SiO_4), coupled with the bilayered structure shown by TEM, suggests that the surface sublayer A mainly contains unreacted Eu_2O_3, since no appreciable Si diffusion occurs in this region. In the interfacial sublayer B the high Si concentration determines a reaction with Eu_2O_3 to form Eu orthosilicate. By increasing the annealing time, the Si diffusion length into the Eu_2O_3 film increases, and Si can therefore more extensively react with Eu_2O_3, as

#160278 - $15.00 USD Received 20 Dec 2011; accepted 3 Feb 2012; published 21 Feb 2012
(C) 2012 OSA

demonstrated by the XRD spectrum of the sample treated at 1000 °C for 300 s in N_2. Eu_2SiO_4-related peaks are still present, but also peaks corresponding to the metasilicate $EuSiO_3$ [19] are found, while peaks corresponding to Eu_2O_3 disappeared.

Since EFTEM measurements (not shown) do not detect any sublayer in this sample, we can reasonably hypothesize the presence of grains of both silicates randomly distributed inside the film. It is strongly remarkable that, in both the silicates detected by XRD (Eu_2SiO_4 and $EuSiO_3$), Eu is in its divalent state, Eu^{2+}, while in the as-deposited film, according to the target composition (Eu_2O_3), almost only Eu^{3+} ions are present. The formation of Eu_2SiO_4 and $EuSiO_3$ is in agreement with the EuO/SiO_2 phase diagram [20]. $Eu^{3+} \rightarrow Eu^{2+}$ reduction in glasses is accomplished by exploiting gaseous reactants such as H_2 [21] or CO [22]; in our case, Eu^{3+} reduction is reasonably due to a solid-state reaction involving the elemental Si (which, in turn, is oxidized) diffusing inside the Eu_2O_3 film.

Figure 3 shows the RT PL spectrum of an as-deposited Eu_2O_3 film; according to literature [6,7,23,24], the spectrum consists of a sharp (full width at half maximum (FWHM) of about 10 nm) main peak at 622 nm, corresponding to the $^5D_0 \rightarrow {}^7F_2$ transition, and of less intense peaks centered at 595, 654 and 709 nm, corresponding to $^5D_0 \rightarrow {}^7F_1$, $^5D_0 \rightarrow {}^7F_3$ and $^5D_0 \rightarrow {}^7F_4$ transitions of Eu^{3+} ions, respectively. Figure 3 also demonstrates that an annealing process at 1000 °C for 30 s in O_2 increases by about a factor of 2 the PL signal attributed to the $^5D_J \rightarrow {}^7F_J$ transitions, due to the presence of a more ordered crystalline environment for the Eu^{3+} ions and to an optimized stoichiometry. No relevant changes of the PL peak shape and intensity occurs by varying the temperature (up to 1000 °C) of the annealing process in O_2 ambient.

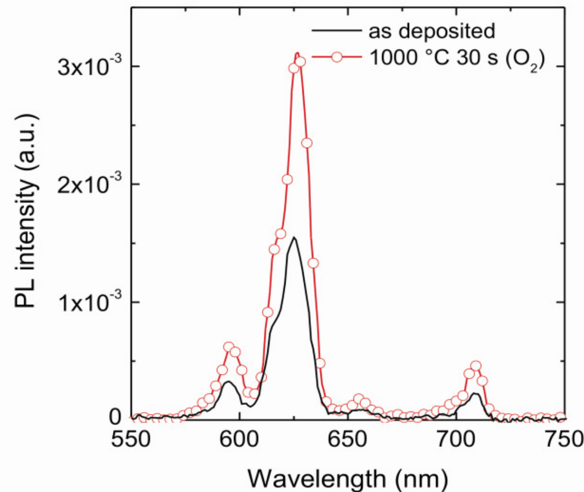

Fig. 3. Room temperature PL spectra obtained by exciting with the 325 nm line of a He-Cd laser Eu_2O_3 films as-deposited and annealed at 1000 °C for 30 s in O_2.

On the other hand, N_2-treated samples show completely different optical properties. Figure 4 reports the RT PL spectra of Eu_2O_3 samples annealed at 1000 °C in N_2 ambient for times ranging from 1 to 300 s; a very bright emission, consisting of a broad band (FWHM of about 95 nm), having the maximum at about 590 nm, is observed. This emission is due to the $4f^65d \rightarrow 4f^7$ transitions of Eu^{2+} ions [9,22,23]. These transitions are dipole-allowed and produce a stronger PL intensity (by more than three orders of magnitude) if compared with the forbidden intra-4f transitions characterizing Eu^{3+} ions.

Received 20 Dec 2011; accepted 3 Feb 2012; published 21 Feb 2012
27 February 2012 / Vol. 20, No. 5 / OPTICS EXPRESS 5505

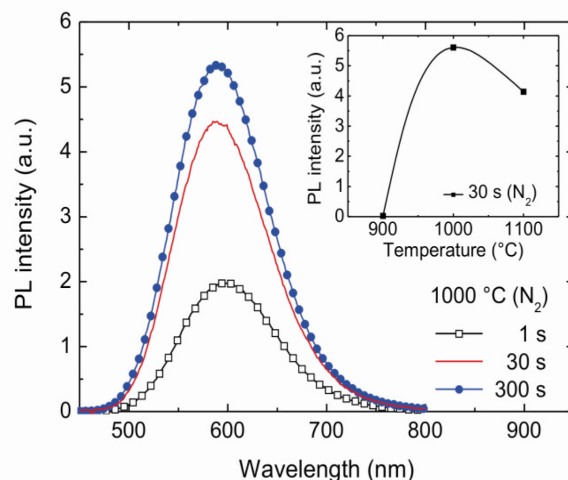

Fig. 4. Room temperature PL spectra obtained by exciting with the 325 nm line of a He-Cd laser Eu_2O_3 films annealed at 1000 °C in N_2 for times ranging from 1 to 300 s. The inset shows the dependence of the integrated PL intensity on the annealing temperature for processes performed for 30 s in N_2.

The Eu^{2+}-related PL intensity increases by increasing the annealing time. We have also explored the dependence of the PL intensity on the annealing temperature for a fixed annealing time of 30 s; the data are reported in the inset of the figure and demonstrate that 1000 °C is the temperature that maximize the PL emission efficiency. We strongly underline that the external quantum efficiency of the brightest N_2-treated Eu_2O_3 samples has been measured to be about 10%, which makes this material of great interest for photonic applications.

The excitation properties of Eu_2O_3 films have been investigated by PLE measurements reported in Fig. 5. PLE spectra were obtained by integrating the PL peaks of the samples and changing the excitation wavelength in the 250-500 nm range. The PLE spectrum of the as-deposited sample exhibits an intense excitation band for wavelengths lower than 300 nm, due to charge transfer transitions [6,7,23]. These findings hold for all samples exhibiting an Eu^{3+} emission. On the other hand, N_2-treated samples (in particular refers to an annealing at 1000 °C for 300 s) exhibit the typical PLE spectrum of Eu^{2+}, characterized by a very intense and broad excitation band centered at about 350 nm, due to $4f^65d\rightarrow4f^7$ transitions [22,23].

The intriguing dependence on the annealing process of the PL properties of Eu_2O_3 can be fully explained by the above discussed TEM and XRD structural data. As-deposited and O_2-treated films are essentially pure Eu_2O_3 and, accordingly, exhibit the typical red emission of Eu^{3+} ions. On the other hand, the Eu^{2+} silicates formed in N_2-treated films exhibit a broader and much more intense PL signal. The possible co-existence of Eu^{2+} and Eu^{3+} in N_2-annealed films remains a partially open question. Residual Eu_2O_3 is still detected in the XRD spectrum of the film annealed for 30 s, but, given the extremely different PL efficiency of the two Eu species and the overlap of the corresponding PL spectra, it is not surprising the absence of any Eu^{3+} contribution to the PL spectrum which is covered by the overwhelming Eu^{2+} contribution. This is even more obvious in the case of the annealing for 300 s, where no XRD peak relative to Eu^{3+} was detected. We remark also that no Eu^{3+} PL signal has been obtained by using an excitation wavelength of 275 nm, corresponding to an enhanced excitation efficiency for Eu^{3+} by about a factor of 30. Therefore, although the occurrence of the almost complete $Eu^{3+}\rightarrow Eu^{2+}$ reduction suggested by XRD is a reasonable hypothesis, the presence of crystalline Eu^{3+} compounds concentrations below the detection limit of XRD, as well as of

#160278 - $15.00 USD Received 20 Dec 2011; accepted 3 Feb 2012; published 21 Feb 2012
(C) 2012 OSA

amorphous Eu^{3+} compounds, cannot be excluded a priori, also in the absence of any optical evidence.

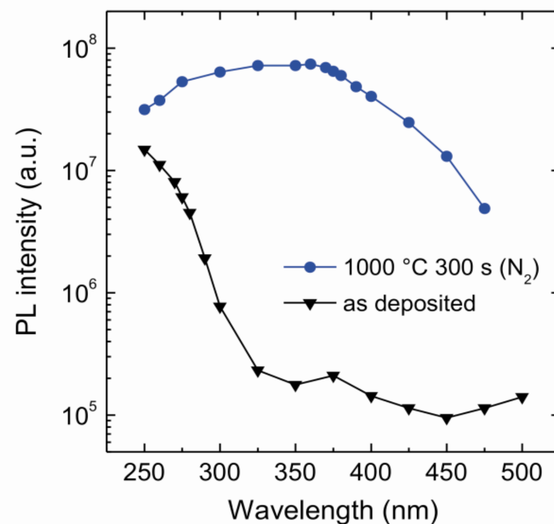

Fig. 5. Room temperature PLE spectra of Eu_2O_3 films as-deposited and annealed at 1000 °C for 300 s in O_2. The spectra were taken by integrating the PL peaks obtained for different excitation wavelengths.

4. Conclusion

In conclusion, we have demonstrated that it is possible, through the control of the Eu oxidation state, to obtain a very strong RT PL emission from Eu-containing thin films deposited on Si substrates. In particular, a stable $Eu^{3+} \rightarrow Eu^{2+}$ reduction has been simply accomplished, and a very high external quantum efficiency (about 10%) has been measured. This is due from one hand to the fact that Eu^{2+} is more easily and efficiently excitable than Eu^{3+} through a broad excitation band, from the other to the observation that Eu^{2+} radiative transitions are dipole-allowed. These properties open the way to promising perspectives for photonic applications of Eu-based materials.

Acknowledgments

The authors thank the CNR-IMM (Catania, Italy) for the use of their TEM facilities.

#160278 - $15.00 USD
Received 20 Dec 2011; accepted 3 Feb 2012; published 21 Feb 2012
(C) 2012 OSA